Super-transition-arrays: A model for the spectral analysis of hot, dense plasma

A. Bar-Shalom
Nuclear Research Center–Negev, P.O. Box 9001, Beer Sheva 84190, Israel

J. Oreg* and W. H. Goldstein
Lawrence Livermore National Laboratory, Livermore, California 94550

D. Shvarts
Nuclear Research Center–Negev, P.O. Box 9001, Beer Sheva 84190, Israel

A. Zigler
Soreq Nuclear Research Center, Yavne 70600, Israel
(Received 21 February 1989)

A method is presented for calculating the bound-bound emission from a local thermodynamic equilibrium plasma. The total transition array of a specific single-electron transition, including all possible contributing configurations, is described by only a small number of super-transition-arrays (STA's). Exact analytic expressions are given for the first few moments of an STA. The method is shown to interpolate smoothly between the average-atom (AA) results and the detailed configuration accounting that underlies the unresolved transition array (UTA) method. Each STA is calculated in its own, optimized potential, and the model achieves rapid convergence in the number of STA's included. Comparisons of predicted STA spectra with the results of the AA and UTA methods are presented. It is shown that under certain plasma conditions the contributions of low-probability transitions can accumulate into an important component of the emission. In these cases, detailed configuration accounting is impractical. On the other hand, the detailed structure of the spectrum under such conditions is not described by the AA method. The application of the STA method to laser-produced plasma experiments is discussed.

I. INTRODUCTION

The unresolved transition array (UTA) model introduced by Bauche, Bauche-Arnoult, and Klapisch[1] presented atomic spectroscopists with a powerful new method for characterizing hot plasma. The model interprets the unresolved spectroscopic structures often observed in laser-produced plasma experiments, as a superposition of many overlapping, Doppler-broadened emission lines. Distinct features correspond to transitions between pairs of electron configurations. Each configuration-configuration transition array is then characterized by average quantities that are obtained analytically, such as total intensity, average transition energy, variance and, in principle, any higher moment of the spectral distribution. (The same problem has been treated by Bloom and Goldberg,[2] using a collective-vector approach.) The sole approximation made in applying the UTA model to plasma emission is that population is distributed statistically amongst the terms of an emitting configuration. This assumption is appropriate to hot, dense plasma, where collisional population transfer is efficient, and the Boltzmann factor is nearly constant, within a configuration.

The UTA model is an efficient solution to the problem of unresolved spectral structures when a relatively small number of atomic configurations are significantly populated. But the model becomes intractable in hot plasmas at high density, where local thermodynamic equilibrium (LTE) is approached, since the number of emitting configurations, and thus the number of calculations required in applying the UTA model, becomes immense. This situation is demonstrated by the spatially integrated spectrum in Fig. 1, obtained in a typical laser-produced plasma experiment.[3] Here, relatively resolved structure, consisting of individual lines and UTA's, sits atop a broad background. The discernible features originate in lower-density regions of the plasma, while the unresolved background is attributable to a dense, LTE emitting region.

The average-atom (AA) model[4] is presently the only tractable approach to analyzing unresolved LTE emis-

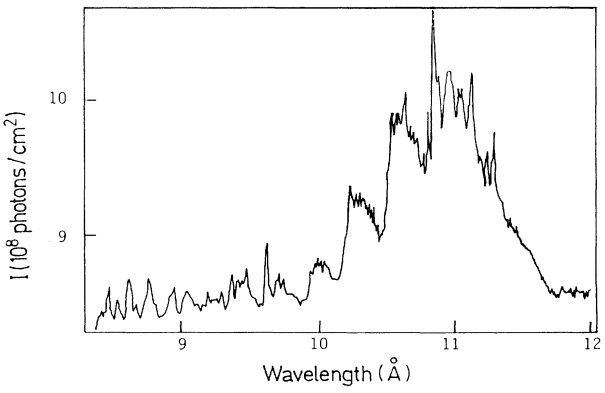

FIG. 1. Emission spectrum of Pr in a laser-produced plasma (Ref. 3).

sion. In this model the transition array moments can be analytically summed, including in each one-electron transition array the contributions of all configurations and charge states in the plasma. The price paid for this striking simplicity is that all these contributions must be computed in a *single potential* and end up subsumed in a *single-Gaussian* spectra distribution. Since many configurations in many charge states contribute to an array, the accuracy of the first approximation is problematic and there is no possibility of its being controlled or tested. The latter approximation entails a total loss of the spectral structure that is typically observed, as in Fig. 1.

In this paper we present a new technique for the modeling and analysis of unresolved plasma emission that introduces the concept of a super-transition-array (STA). This is a transition array between "superconfigurations" that contain many ordinary configurations lying sufficiently near in energy to be accurately treated in a common potential. In this approach, the single potential and Gaussian of the AA model is replaced by a superposition of Gaussians that can reveal the internal structure of an array when it exists, each computed in its own, more accurate, potential. On the other hand, the number of transition arrays for which the moments must be calculated is reduced by many orders of magnitude from what is required in directly summing configuration UTA's. The STA technique is a general approach that interpolates smoothly between the AA and UTA models, which reappear as special cases. It is applicable where the UTA model proves too detailed, but the AA model is an oversimplification.

In the next section, we introduce several concepts and definitions required to derive and apply the STA model. In Sec. III, STA's are defined and a representation for their moments is derived in terms of "generalized" partition functions. These partition functions are explicitly evaluated using recursion relations in Sec. IV, to obtain explicit formulas for the various moments of an STA.

In Sec. V, the STA model is compared with the AA and UTA results in a simple case, and then applied to a laser-produced plasma experiment. The STA spectrum is constructed for plasma conditions determined by a hydrodynamic simulation code[5] and then compared to the observed emission. A discussion and summary of our results is given in Sec. VI.

II. DEFINITIONS AND THEORETICAL BACKGROUND

A. Spontaneous-emission transition arrays

We define a spontaneous-emission transition array as the spectral distribution of photons emitted in transitions between two groups of levels, A and B:[1]

$$S_{AB}(E)=\sum_{a\in A,b\in B} N_a A_{ab} P(E-E_{ab}) , \tag{1}$$

where $P(E-E_{ab})$, the normalized line profile, is assumed to be equal for all transitions, and

$$A_{ab}=kE_{ab}^3 d_{ab} \tag{2}$$

is the Einstein coefficient for spontaneous emission,[6] with

$$k=(8\pi^2 e a_0)^2/3h^4c^3 \tag{3}$$

and the dipole reduced matrix element,[7]

$$d_{ab}=\left|\left\langle a\left|\left|\sum_i r_i\right|\right|b\right\rangle\right|^2 \Big/ g_a . \tag{4}$$

N_a and g_a are the population density and statistical weight, respectively, of the initial level.

When the $A\rightarrow B$ transitions form a distinct unresolved pattern, its shape can be characterized by the first few moments of the spectral distribution:[1]

$$\mu^{(n)}=\frac{\int S_{AB}(E)E^n dE}{\int S_{AB}(E)dE} . \tag{5}$$

In terms of these array moments, the average transition energy is $\mu^{(1)}\equiv E_{AB}$; the variance is

$$\mu^{(2)}-(\mu^{(1)})^2\equiv(\Delta E_{AB})^2 ,$$

etc.

In hot plasma, the width of the line profile $P(E-E_{ab})$ is negligible compared to the width of the total array and it can be replaced by a δ function, yielding

$$\mu^{(n)}=\frac{\sum_{a\in A,b\in B} N_a d_{ab} E_{ab}^3 E_{ab}^n}{\sum_{a\in A,b\in B} N_a d_{ab} E_{ab}^3} \cong \frac{\sum_{a\in A,b\in B} N_a d_{ab} E_{ab}^n}{\sum_{a\in A,b\in B} N_a d_{ab}} , \tag{6}$$

where we have approximated A_{ab} by

$$A_{ab}=kE_{AB}^3 d_{ab} . \tag{7}$$

The total photon intensity of the array is given by

$$I_{AB}=k\sum_{a\in A,b\in B} N_a d_{ab}(E_{ab})^3 \cong k(E_{AB})^3 \sum_{a\in A,b\in B} N_a d_{ab} . \tag{8}$$

A special case of the general definition given here is the j-j configuration transition array. This covers transitions between the levels contained in a pair of j-j configurations, C and C', that we can denote by

$$C=\prod_s \mathbf{j}_s^{q_s}, \quad C'=\prod_s \mathbf{j}_s^{q_s'} , \tag{9}$$

where q_s and q_s' are the electron occupation numbers of the shell $\mathbf{j}_s\equiv\{n_s,l_s,j_s\}$ (for nonrelativistic configurations $\mathbf{j}_s\equiv\{n_s,l_s\}$). A *specific* one-electron transition from orbital $\mathbf{j}_\alpha$ to $\mathbf{j}_\beta$ will be denoted by $\alpha\rightarrow\beta$. In this case, $q_\alpha'=q_\alpha-1$, $q_\beta'=q_\beta+1$, $q_s'=q_s$, $s\neq\alpha,\beta$. The general formulas introduced above apply to the configuration array, with the obvious substitution of C and C' for A and B.

The UTA model[1] is based on the configuration transition array, with the added approximation that the level populations N_a of the upper configuration are related to

each other by statistics, i.e., by relative multiplicity. This assumption allows Eqs. (6) and (8) to be evaluated analytically.

The collection of all configuration transition arrays with specific $\alpha \rightarrow \beta$ form the total one-electron transition array for that transition. It is clear that this collection can become very large when the contributions of all possible spectator electron configurations in all charge states are included. In non-LTE plasma, few of these configurations and charge states are heavily enough populated to contribute significant emission, and the configuration-by-configuration approach of the UTA model is sufficient. It is the one-electron transition array under LTE conditions, where the number of configurations yielding non-negligible contributions is immense, that we propose to treat by the STA model.

B. LTE plasma conditions

Under LTE conditions, not only are the level populations within a configuration statistically distributed (assuming a constant Boltzmann factor), but the relative populations of any two groups of levels are related by the ratio of their partition functions. Thus the ionization balance is determined by the Saha equation,

$$\frac{N_Q}{U_Q} = \frac{N}{U} , \tag{10}$$

where N_Q is the partial density of ions with Q electrons, and

$$U_Q = e^{Q\mu/kT} \sum_a g_a e^{-E_a/kT} \tag{11}$$

is the ionic partition function at plasma chemical potential μ. The total ion density and partition function are, respectively,

$$N = \sum_Q N_Q , \tag{12}$$

$$U = \sum_Q U_Q . \tag{13}$$

The sum in Eq. (11) is over all atomic energy levels E_a of charge state Q. Although it is formally infinite, the sum is actually truncated for ions in plasma by continuum lowering.[8] This effect leads to a reduction of the ionization potential, and, thus, a maximum principal quantum number $n_{\max}$ above which an electron is not bound. In our calculations, we will use the ion sphere model[8] to estimate $n_{\max}$. This model does not include plasma effects on the potential except for lowering of the ionization potential. However, the theory developed in the present work is applicable for any potential.

Clearly, Eq. (10) can apply also to any subset P of levels within a charge state, when N_Q and U_Q are replaced by the corresponding density and partition function N_P and U_P of the subset. This case will be essential to the development of super-transition-arrays.

It is well known that a profound simplification of the partition function (11) is obtained in the non-interacting limit, where E_a is a sum of single-particle energies. In atomic physics, this approximation is equivalent to using zero-order configuration-average energies,

$$E_C^{(0)} = \sum_{s \in C} q_s \varepsilon_s , \tag{14}$$

where ε_s is the energy of an electron in shell s. (It is possible to obtain a "best," or perturbation-theory-improved, value for $E_C^{(0)}$, and this is discussed in Appendix B.) Use of this 'best" zero-order approximation in the Boltzmann factor that appears in partition functions is crucial to the STA method. A detailed justification will be elaborated in the discussion in Sec. VI.

Using Eq. (14), we can rewrite the ion's partition function as

$$U_Q = \sum_{\sum_s q_s = Q} \prod_s \begin{bmatrix} g_s \\ q_s \end{bmatrix} X_s^{q_s} , \tag{15}$$

where

$$X_s = e^{-(\varepsilon_s - \mu)/kT} . \tag{16}$$

The sum in Eq. (15) is over sets of orbital occupation numbers $\{q_s\}$ that obey the constraint $\sum_s q_s = Q$. This sum can, of course, be further restricted, so that U_Q refers to a subset of configurations, rather than an entire charge state.

III. SUPER-TRANSITION-ARRAYS

The problem in applying transition array methods to LTE plasma emission spectra is that a huge number of configurations, from a range of charge states, contribute to each specific one-electron transition. For charge state Q, these configurations arise from all possible partitions of the $Q-1$ spectator electrons among the shells in Eq. (9). All of these partitions will lead to transitions in a common spectral region. The occurrence of $n_{\max} > 10$ for typical laser-produced plasma gives rise to over 10^{15} configuration-configuration contributions to any particular one-electron transition. Although many of these involve high-lying levels with small Boltzmann factors, their large statistical weights and shear abundance easily accumulate to a significant contribution. This proliferation of configurations can be handled by grouping them into "superconfigurations," and defining a super-transition-array as the collection of all the possible transitions between a pair of superconfigurations. We will demonstrate that, under LTE conditions, where each configuration is populated according to an equation analogous to (10), the moments of an STA, like those of a UTA, can be obtained in closed form.

A. Definitions and general expressions

An STA is defined as the collection of *all* transitions between a pair of superconfigurations characterized by the same one-electron excitation ($\alpha \rightarrow \beta$). A superconfiguration comprises many individual configurations. These can be chosen arbitrarily but, in general, the choice will be motivated by physical considerations, such as en-

ergetic propinquity. Using a nonrelativistic description, a general superconfiguration can be expressed symbolically as

$$\Xi \equiv \prod_{\sigma} \left[\prod_{s_\sigma} n_{s_\sigma} l_{s_\sigma} \right]^{k_\sigma} . \tag{17}$$

Here, the term in large parentheses, indexed by σ, defines a supershell. The fixed occupation number of each supershell is k_σ and the index s_σ runs over all the shells in the supershell σ. The superconfiguration is the collection of ordinary configurations obtained by distributing the k_σ electrons to the shells of the supershell σ in all possible ways (consistent with the Pauli principle, of course).

As a simple example, we consider the neonlike superconfiguration

$$\Xi_{\mathrm{Ne}} = (1s)^2(2s2p)^7(3s3p3d4s4p4d4f)^1 . \tag{18}$$

Ξ_{Ne} comprises 14 configurations (36 j-j configurations) and 88 levels. Clearly this multiplicity increases geometrically as electrons (or holes) are added to supershells. For example, to describe the emission from LTE plasma in the spectral region of transitions between Ξ_{Ne} and the Ne-like ground state, we must include also transitions involving a spectator electron in the third supershell:

$$\Xi'_{\mathrm{Ne}} = (1s)^2(2s2p)^6(3s3p3d4s4p4d4f)^2, \tag{19a}$$

$$\Xi_{\mathrm{Na}} = (1s)^2(2s2p)^7(3s3p3d4s4p4s4f)^2 . \tag{19b}$$

Already at this level of complication, the superconfigurations Ξ'_{Ne} and Ξ_{Na} comprise 864 and 432 individual j-j configurations, respectively.

The moments of the STA are given in terms of Eq. (6), with A and B referring to any particular superconfigurations. We assume, in common with the UTA model, that the total population in any ordinary configuration is distributed statistically among its levels. The approximation of a constant Boltzmann factor over each configuration is appropriate to hot plasma emission. Note, however, that we *do not* assume a constant Boltzmann factor over a superconfiguration, but allow instead a thermal distribution of population among its configurations. We also take level energies by their first-order configuration averages. This effectively allows us to treat the configurations within a superconfiguration on a level equivalent to the levels of an ordinary configuration.

From Eqs. (6) and (8) we can obtain the average energy, variance, and total intensity of an STA for the one-electron $\alpha \rightarrow \beta$ transition:

$$E_{\alpha\beta} = \mu^{(1)}(\alpha,\beta) = \frac{\sum_{C\in\Xi} N_C d_C^{(\alpha\beta)} E_C^{(\alpha\beta)}}{\sum_{C\in\Xi} N_C d_C^{(\alpha\beta)}} , \tag{20}$$

$$\Delta E^2_{\alpha\beta} = \frac{\sum_{C\in\Xi} N_C d_C^{(\alpha\beta)} (E_C^{(\alpha\beta)} - E_{\alpha\beta})^2}{\sum_{C\in\Xi} N_C d_C^{(\alpha\beta)}} , \tag{21}$$

$$I_{\alpha\beta} = \sum_{C\in\Xi} I_{CC'} = k E^3_{\alpha\beta} \sum_{C\in\Xi} N_C d_C^{(\alpha\beta)} , \tag{22}$$

where the sums are over all configurations C that are contained in the superconfiguration Ξ, and include at least one electron in orbital α and one hole in orbital β, and C' is determined uniquely from C by the $\alpha \rightarrow \beta$ transition.

The quality $d_C^{(\alpha\beta)}$ is the configuration average of the dipole reduced matrix element defined in Eq. (4):

$$d_C^{(\alpha\beta)} = \sum_{a\in C, b\in C'} g_a d_{ab} \Big/ \sum_{a\in C} g_a = q_\alpha (g_\beta - q_\beta)(r_{\alpha\beta})^2 , \tag{23}$$

with $r_{\alpha\beta} = \langle \alpha \| r \| \beta \rangle$ and $q_\alpha, g_\beta - q_\beta$, respectively, the number of electrons and holes in orbitals α and β of configuration C. $E_C^{(\alpha\beta)}$ is the first-order average transition energy between C and C'. Its dependence on α,β and the shell occupation numbers of C is presented in Appendix C. [Note that $E_C^{(\alpha\beta)}$ has replaced $E_{ab}, a\in C, b\in C'$ in Eq. (6)]. It should be noticed also that Eq. (20) for the average energy is obtained from Eq. (6) with no approximation, whereas in Eq. (21) for the variance the width of each configuration can also be taken into account exactly but we have neglected it here compared to the STA total width.

Under our LTE assumption, N_C, the total configuration population, is given by the Saha-like equation

$$N_C = \frac{N_Q \sum_{a\in C} g_a e^{-(E_a - Q\mu)/kT}}{\sum_{\text{all } C} \sum_{a\in C} g_a e^{-(E_a - Q\mu)/kT}} \approx (N_Q/U_Q) g_C e^{-(E_C - Q\mu/kT} . \tag{24}$$

We have neglected the spread in level energies compared to kT, within configuration C, here, in introducing the configuration-average energy E_C.

From Eqs. (20)–(23) it is clear that configurations play much the same role in STA's as do levels in UTA's. This coarser level of averaging is one of the keys to treating the vast number of configurations that radiate in LTE. But the analogy fails in a crucial detail: in the STA model the distribution of population among configurations is thermal and not statistical. It is necessary to retain the Boltzmann form for N_C precisely because it cannot be assumed that the range of energies E_C within a superconfiguration is small compared to kT. There is a further, practical, difference: for superconfigurations, the number of terms in the sums over C easily becomes enormous, as opposed to the more measured proliferation of levels in a configuration UTA. In the following sections, we show that both of these complications are tractable.

B. The moments in terms of formal partition functions

The first step in reducing the STA model to a useful tool is to render the moments, Eqs. (20)–(22), in terms of "formal" partition functions of the form in Eq. (15). (The meaning of "formal" will be clarified below.) We will then show that these formal partition functions can be evaluated analytically using recursion relations.

Following the discussion leading up to Eq. (15), we adopt the approximation of using the "best" zeroth-order configuration-average energy in the Boltzmann factors of the moments. This gives

$$I_{\alpha\beta}=k(N/U)E_{\alpha\beta}^3\begin{bmatrix} j_\alpha & 1 & j_\beta \\ \frac{1}{2} & 0 & -\frac{1}{2}\end{bmatrix}^2 r_{\alpha\beta}^2 W^{(\alpha\beta)} , \tag{25}$$

$$E_{\alpha\beta}=\sum_C w_C^{(\alpha\beta)}E_C^{(\alpha\beta)}/W^{(\alpha\beta)} , \tag{26}$$

$$\Delta E_{\alpha\beta}^2=\sum_C w_C^{(\alpha\beta)}(E_C^{(\alpha\beta)}-E_{\alpha\beta})^2/W^{(\alpha\beta)} , \tag{27}$$

where

$$w_C^{(\alpha\beta)}=q_\alpha(g_\beta-q_\beta)\prod_{s\in C}\begin{bmatrix} g_s \\ q_s\end{bmatrix}X_s^{q_s} , \tag{28}$$

$$W^{(\alpha\beta)}=\sum_C w_C^{(\alpha\beta)}=X_\alpha g_\alpha g_\beta U_{Q-1}(\mathbf{g}^{\alpha\beta}) , \tag{29}$$

and the 2×3 matrix in Eq. (25) is a 3-j symbol. In Eq. (29), $U_{Q-1}(\mathbf{g}^{\alpha\beta})$ is defined by Eq. (15), generalized such that the set of statistical weights appearing there is given by

$$\mathbf{g}^{\alpha\beta}=\{g_1,g_2,\ldots,g_{s-1},g_s-\delta_{\alpha s}-\delta_{\beta s},g_{s+1},\ldots\} . \tag{30}$$

That is, in the "formal" partition function entering Eq. (29), the statistical weight of shells α and β are reduced by one from their physical values. In deriving (29) we have also made use of the binomial relations:

$$q\begin{bmatrix} g \\ q\end{bmatrix}=g\begin{bmatrix} g-1 \\ q-1\end{bmatrix} ,$$
$$(g-q)\begin{bmatrix} g \\ q\end{bmatrix}=g\begin{bmatrix} g-1 \\ q\end{bmatrix} . \tag{31}$$

The expression for the first-order average transition energy between the configurations C and C' is[1]

$$E_C^{(\alpha\beta)}\equiv E_{CC'}=\sum_{s\in C}(q_s-\delta_{s\alpha})+D_s+D_0 , \tag{32}$$

where D_s and D_0 are independent of q_s and can be obtained in terms of the Slater integrals $F^{(k)}(\alpha,\beta),G^{(k)}(\alpha,\beta)$ (see Appendix C) and s runs over all shells in C.

These relations lead to the following expressions for the moments of the super array:

$$I_{\alpha\beta}=k(N/U)E_{\alpha\beta}^3\begin{bmatrix} j_\alpha & 1 & j_\beta \\ \frac{1}{2} & 0 & -\frac{1}{2}\end{bmatrix}^2 r_{\alpha\beta}^2 X_\alpha g_\alpha g_\beta U_{Q-1}(\mathbf{g}^{\alpha\beta}), \tag{33}$$

$$E_{\alpha\beta}=\sum_{\{\sum_s q_s=Q\}}\left[\begin{bmatrix} g_s-\delta_{s\alpha}-\delta_{s\beta} \\ q_s-\delta_{s\alpha}\end{bmatrix}X_s^{q_s-\delta_{s\alpha}}\right]\frac{\sum_r(q_r-\delta_{r\alpha})\mathbf{D}_r+\mathbf{D}_0}{U_{Q-1}(\mathbf{g}^{\alpha\beta})}$$
$$=D_0+\sum_r D_r X_r g_r^{\alpha\beta}U_{Q-2}(\mathbf{g}^{\alpha\beta r})/U_{Q-1}(\mathbf{g}^{\alpha\beta}) , \tag{34}$$

where $g_r^{\alpha\beta}=g_r-\delta_{\alpha r}-\delta_{\beta r}$,

$$\mathbf{g}^{\alpha\beta r}=\{g_1,g_2,\ldots,g_{s-1},g_s-\delta_{\alpha s}-\delta_{\beta s}-\delta_{sr},g_{s+1},\ldots\} \tag{35}$$

and

$$\Delta E_{\alpha\beta}^2=\left[\sum_{t,r}(D_t X_t g_t^{\alpha\beta})(D_r X_r g_r^{\alpha\beta s})U_{Q-3}(\mathbf{g}^{\alpha\beta\mathrm{tr}})+\sum_t(D_t^2 X_t g_t^{\alpha\beta})U_{Q-2}(\mathbf{g}^{\alpha\beta t})\right]\Big/U_{Q-1}(\mathbf{g}^{\alpha\beta})-(E_{\alpha\beta}-D_0)^2 , \tag{36}$$

where

$$\mathbf{g}^{\alpha\beta\mathrm{tr}}=\{g_1,g_2,\ldots,g_{s-1},g_s-\delta_{\alpha s}-\delta_{\beta s}-\delta_{st}-\delta_{sr},g_{s+1}\ldots\} . \tag{37}$$

Eqs. (33), (34), and (36) represent the STA moments in terms of formal partition functions with no further approximations than the use of zeroth-order configuration-average energies in the Boltzmann factors. The problem that remains is to compute the partition functions. Clearly, though, this will involve summation over enormous numbers of terms. One solution to this problem is the average-atom model, and before presenting a new approach, we review this model and its limitations in the next section. We will then describe our STA results which overcome the limitations of the average atom while retaining its simplicity.

C. The average-atom model

In the average-atom model all the contributions from *all configurations in all ionization stages* constituting a single, total one-electron transition array, are accounted for using a single set of one-electron orbital energies. The

moments of this array are obtained by summing over all Q in Eqs. (33), (34), and (36). Since the single-electron energies are independent of Q, the total partition function of the system can be evaluated:

$$U=\sum_{Q} U_Q=\sum_{Q}\sum_{\{\sum_s q_s=Q\}}\prod_s \begin{bmatrix} g_s \\ q_s \end{bmatrix} X_s^{q_s}$$

$$=\prod_s \sum_{q_s=0}^{g_s} \begin{bmatrix} g_s \\ q_s \end{bmatrix} X_s^{q_s}=\prod_s (1+X_s)^{g_s} , \tag{38}$$

where we have used the sum over Q to remove the restriction $\sum_s q_s=Q$ and obtain a product of independent sums over shells s. Thus, in the average-atom model, the moments of the total transition array reduce to

$$E_{\alpha\beta}=D_0+\sum_r D_r X_r g_r^{\alpha\beta}\prod_s (1+X_s)^{g_s^{\alpha\beta r}} \Big/ \prod_s (1+X_s)^{g_s^{\alpha\beta}}$$

$$=D_0+\sum_r D_r n_r g_r^{\alpha\beta} \tag{39}$$

and

$$\Delta E_{\alpha\beta}^2=\sum_r D_r^2 g_r^{\alpha\beta} n_r(1-n_r) , \tag{40}$$

where

$$n_r=X_r/(1+X_r)=[1+\exp(\varepsilon_r-\mu)/kT]^{-1} \tag{41}$$

is the Fermi-Dirac population probability for the single-electron energy level ε_r. Equations (39)–(41) reproduce the results of Ref. 4, where they were derived from purely statistical considerations.

This derivation shows that the sum over the immense number of terms in Eqs. (34) and (35) can be carried out in the average-atom approximation, yielding the average-atom formulas that contain summations only over shells (numbering a few tens). The price paid for this striking simplification is that the entire one-electron transition array is represented by a single Gaussian with no additional structure. Furthermore, since only one set of orbitals serves for all configurations in all ionization stages the accuracy of this Gaussian is highly circumscribed.

To improve on the average-atom approximation, one must perform the sum over a limited set of transitions, rather than the entire one-electron array. Each separate sum, or super-transition-array, forms a distinct Gaussian, and different orbital energies can be used in each STA. Thus the moments of each STA are more accurate, and, depending on how the set of STA's is chosen, the model will reveal as much spectral structure as required. In the next section we show how the STA model can be easily applied using recursion formulas for the formal partition functions. These produce simple analytical expressions for the STA moments and eliminate the extremely laborious summations.

IV. RECURSION FORMULAS FOR THE PARTITION FUNCTION AND WORKING FORMULAS FOR THE MOMENTS OF AN STA

The partition function of a superconfiguration is obviously the product of the partition function for its occupied supershells. In Appendix A we derive the following recursion formulas for the partition functions for a supershell σ having Q_σ electrons:

$$U_0(\mathbf{g})=1 ,$$
$$U_{Q_\sigma}(\mathbf{g})=\sum_{n=1}^{Q_\sigma} \chi_n^\sigma U_{Q_\sigma-n}(\mathbf{g})/Q_\sigma , \tag{42}$$

where

$$\chi_n^\sigma=-\sum_{s\in\sigma} g_s(-X_s)^n . \tag{43}$$

For example,

$$U_1(\mathbf{g})=\chi_1^\sigma ,$$
$$U_2(\mathbf{g})=(\chi_1^\sigma U_1+\chi_2^\sigma)/2 , \tag{44}$$

and so on. Thus the partition function for Q_σ electrons is obtained in Q_σ steps. (A similar recursion formula is used in the single-particle ideal-gas model.[9])

In Appendix A we also derive a relation between formal partition functions differing in the value of one of their weights $\mathbf{g}$:

$$U_{Q_\sigma}(\mathbf{g})=U_{Q_\sigma}(\mathbf{g}^\gamma)+X_\gamma U_{Q_\sigma-1}(g^\gamma) \tag{45}$$

where the set $\mathbf{g}^\gamma$ is obtained from $\mathbf{g}$ by reducing the weight of shell γ by 1,

$$\{g_s^\gamma\}=\{g_s-\delta_{\gamma s}\} . \tag{46}$$

Using the formulas (44) and (45), the STA's moments reduce to

$$I_{\alpha\beta}=k(N/U)E_{\alpha\beta}^3 \begin{bmatrix} j_\alpha & 1 & j_\beta \\ \frac{1}{2} & 0 & -\frac{1}{2} \end{bmatrix}^2 r_{\alpha\beta}^2 X_\alpha g_\alpha g_\beta$$
$$\times\prod_\sigma U_{Q'_\sigma}(\mathbf{g}^{\alpha\beta}) , \tag{47}$$

where, here, σ runs over supershells. The charges Q'_σ are given by $Q'_\sigma=Q_\sigma-1$, Q_σ for $\alpha\in\sigma$, $\alpha\notin\sigma$, respectively, and obey the constraint

$$\sum_\sigma Q'_\sigma=Q-1 . \tag{48}$$

The ratio N/U is equal to the corresponding ratio N_Ξ/U_Ξ for each superconfiguration.

The average energy of the STA is given by

$$E_{\alpha\beta}=D_0+\sum_{\sigma=1}^{\mathcal{N}} \mathcal{E}_{\alpha\beta}^\sigma , \tag{49}$$

$$\mathcal{E}^{\sigma}_{\alpha\beta}=\sum_{n=0}^{Q_\sigma}\phi^{\sigma}_{n}(D)U_{Q_\sigma-n}(\mathbf{g}^{\alpha\beta})/U_{Q_\sigma}(\mathbf{g}^{\alpha\beta}) , \tag{50}$$

where $\mathcal{N}$ is the number of supershells, Q_σ is the number of electrons in the supershell σ, and

$$\phi^{\sigma}_{n}(D)=-\sum_{s\in\sigma}g^{\alpha\beta}_{s}D_{-s}(-X_s)^n . \tag{51}$$

In a similar way, we obtain for the variance

$$\Delta E^2_{\alpha\beta}=\sum_{\sigma=1}^{\mathcal{N}}\Delta^{\sigma}_{\alpha\beta} , \tag{52}$$

where

$$\Delta^{\sigma}_{\alpha\beta}=\sum_{n=1}^{Q_\sigma}\eta^{\sigma}_{n}U_{Q_\sigma-n}(\mathbf{g}^{\alpha\beta})/U_{Q_\sigma}(\mathbf{g}^{\alpha\beta})-(\mathcal{E}^{\sigma}_{\alpha\beta})^2 , \tag{53}$$

$$\eta^{\sigma}_{n}=\sum_{m=1}^{n-1}\phi^{\sigma}_{m}(D)\phi^{\sigma}_{m-n}(D)+n\phi^{\sigma}_{n}(D^2) , \tag{54}$$

where $\phi^{\sigma}_{n}(D^2)$ is given by Eq. (51) with D_s^2 replacing D_s.

In the above equations we have taken the "best" zeroth-order energies in the Boltzmann factors. However, these equations are valid also if all the configuration energies are shifted by a constant. This allows us to improve the Boltzmann factors by adding the average first-order correction to the zeroth-order energies of all the configurations within the superconfiguration. Clearly, this correction will not effect the average energy and variance of the STA, but the intensity of each STA and therefore the shape of the total one-electron transition array will be improved. The expression for this correction is given in Appendix B.

V. RESULTS

We have developed a computer code based on the parametric potential atomic structure model[10] to evaluate the working formulas given above. We have used it to illustrate the differences between the AA, UTA, and STA methods, and to demonstrate the advantages of the latter, by working a relatively simple example involving only about 40 000 configurations: not yet so many that an explicit UTA calculation is prohibitively expensive and time-consuming. The example is the transition array $\alpha=3d_{5/2}\rightarrow\beta=2p_{3/2}$ in iron, at solid density and a temperature of 200 eV. For these conditions, the ion sphere model predicts $n_{\max}=4$.

The predictions for this transition array of the average-atom, STA, and UTA methods are shown in Fig. 2. The UTA spectrum, containing the highest level of detail, shows several distinct peaks that are completely missed in the average-atom model. However, the UTA structure is reproduced almost exactly in the STA spectrum, in which only *eight* STA's for each of the charge states included in the example (Fe^{5+}–Fe^{21+}), were used.

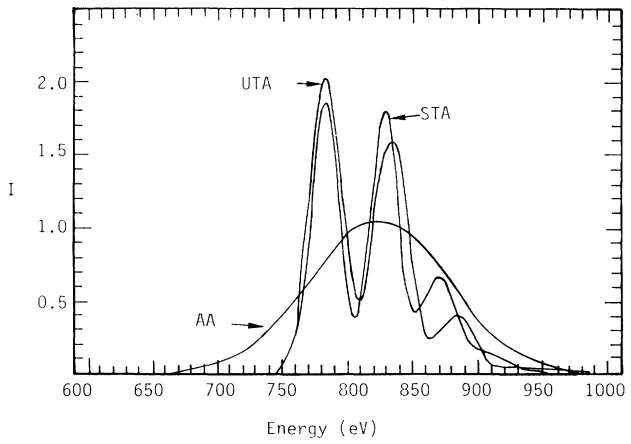

FIG. 2. Comparison of the average-atom, UTA, and STA results for the total one-electron transition array $3d_{5/2}$–$2p_{3/2}$ in iron, at $T_e=200$ eV, $N_I=8.5\times10^{22}$ cm^{-3}. The intensity is in arbitrary units.

Thus the 40 000 Gaussians of the UTA model can be accurately represented by a small number of STA's. We will demonstrate below that even in cases where the number of UTA's exceeds 10^9, and their explicit calculation becomes impractical, still only several tens of STA's are required for an accurate spectrum.

In the iron example, the definition of supershells is guided by simple physical considerations: only shells with similar energies are collected into the same supershell. Thus the large energy gap between the $n=2$ and $n>2$ shells suggested that the superconfigurations be defined as follows:

$$\Xi_{mk}=(1s)^2(2s2p)^m(3s3p3d4s4p4d4f)^k ,$$

where $m=0,1,\ldots,7$ and $k=Q-m$ for each charge state, Q. This choice yielded eight superconfigurations for each charge state. Indeed each peak in Fig. 2 arises from different initial superconfigurations. Further subdivisions of these supershells did not reveal further details of the spectral structure.

In Fig. 3, the accuracy of the moments obtained using the AA method is tested by comparing the AA result for the iron example (trace *a*), with two similar calculations that each involves a single STA [i.e., including all shells in one large supershell: $\Xi_Q\equiv(1s2s2p3s3p3d4s4p4d4f)^Q$] for each charge state. In this comparison, the STA method allows us to choose a separate potential for each charge state. In the STA results, the energy in the Boltzmann factor is calculated in either zeroth-order (trace *b*) or first-order (trace *c*) approximations. The first-order result was obtained by explicitly constructing the STA's moments by summing detailed configuration arrays, an approach made possible only by the small number of contributing configurations. The inaccuracy associated with taking average first-order energy corrections in the Boltzmann factor is clearly much smaller than the effect of using different potential for each STA. The STA result can therefore always be further improved by refining the definition of the

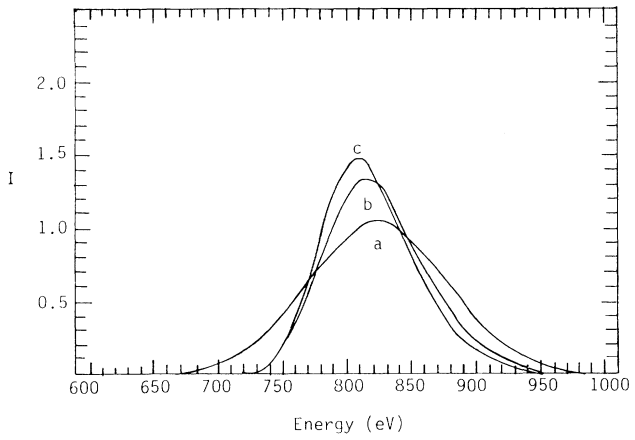

FIG. 3. Effect of the first-order correction to the energy used in the Boltzmann factor of the STA model, for iron under the condition of Fig. 2. Curve *a*, average-atom result (zeroth-order energies); curve *b*, with a single STA for each charge state and zeroth-order energies; and curve *c*, with a single STA for each charge state but using first-order energies.

superconfigurations, to include smaller number of configurations, with its own appropriate potential (see the discussion).

Figure 4 shows STA predictions for the LTE spectrum of Pr in the laser-produced plasma of Fig. 1.[3] The plasma conditions attained in this experiment were obtained using a detailed one-dimensional hydrodynamics code.[5] Since the experimental results are time integrated and include non-LTE contributions from low-density outer regions, we intend this comparison to be suggestive only and have chosen typical temperatures $T_e=200$ eV, $T_e=250$ eV and density of $N_I=10^{20}$ cm^{-3}. Under these conditions, $n_{\max}=12$, but the results are insensitive to small changes in this value. We have successively increased the number of STA's used in this example, by reducing the number of shells in each supershell, until convergence of the spectral structure was achieved. The final set of supershells was

$$(1s)^2(2s2p)^k(3s3p3d)^m(4s4p\cdots n_{\max}l_{\max})^n$$

with $2+k+m+n=Q$ for each charge state Q. The number of superconfigurations thus obtained is a few hundreds.

The sensitivity of the results to the temperature demonstrated in Fig. 4 could serve as a diagnostic in space- and time-resolved plasma experiments.

The one-electron transition that dominates the Pr spectrum is $4f_{7/2}$-$3d_{5/2}$. In Fig. 5 the spectrum of this transition alone is shown for three cases. The STA1 prediction is obtained by combining shells into a single supershell for each charge state, as in the iron example (Fig. 3). Again it is clear that the STA model, even at a minimal level of detail, improves significantly over the average-atom method.

The UTA method takes into account only configurations whose contribution is estimated, *a priori*, to be most significant. Since the STA method can easily include all contributions, it provides a test of this approximation, as well as the means of successively improving upon it. We have found that under certain plasma conditions, contributions estimated individually to be small, and thus neglected in the UTA model, may in fact dominate when they are summed. As an illustration, we calculated the UTA spectrum for a group of 48 configurations that were estimated[11] to dominate the Pr emission at a temperature of 250 eV and a density of 10^{20} ions per cm^3. The partition function for this group turned out to constitute only one-fifth of the total, leading to the striking differences in predicted emission spectra shown in Fig. 6. The trace labeled *b* represents the result of the 48-configuration model, that assumes that all population is distributed among these 48 configurations. The *a* trace is the total contribution of all possible configurations as calculated in the STA model, and the *c* line is the partial contribution, in that model, of the 48

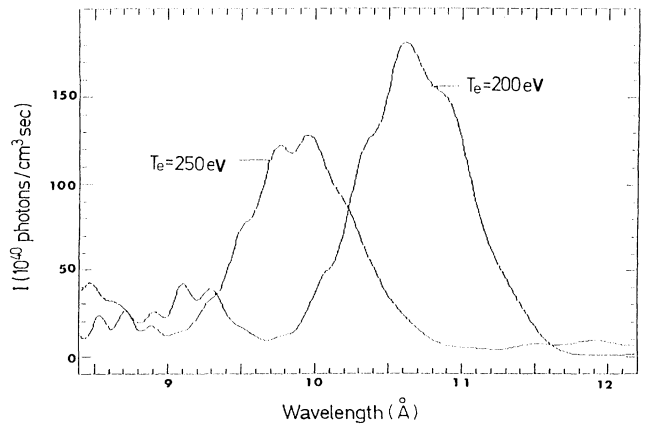

FIG. 4. STA results for the Pr spectrum at LTE with $N_I=10^{20}$ cm^{-3}, $T_e=200$ and 250 eV.

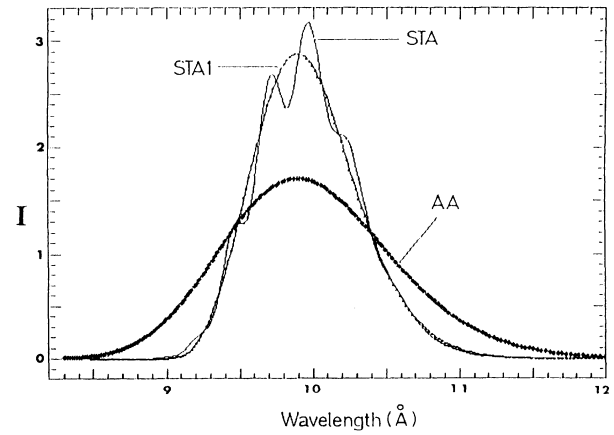

FIG. 5. Emission spectra for the one-electron transition $4f_{7/2}$–$3d_{5/2}$ in Pr at $N_I=10^{20}$ cm^3 and $T_e=250$ eV. AA, average atom; STA, convergence with increasing number of STA's; STA1, single supershell for each charge state.

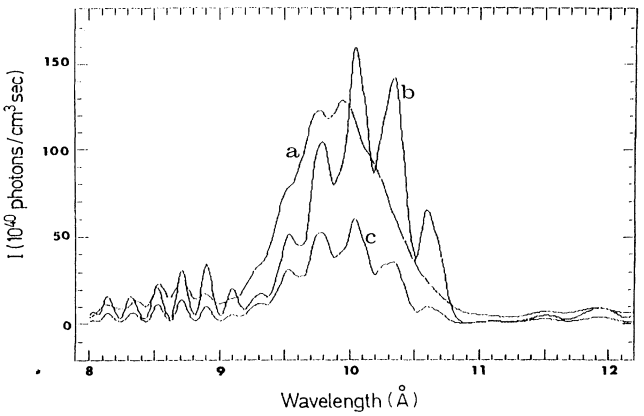

FIG. 6. Comparison between (curve *a*) the converged STA spectrum, and the spectrum obtained by a detailed calculation involving only the 48 configurations expected to dominate the emission, with (curve *b*) this contribution normalized to its own partition function for each charge state, or (curve *c*), normalized to the total partition function in each charge state.

configurations.

The difference between the *a* and *b* lines demonstrates that the contribution of all the configurations excluding the 48 main configurations cannot be accounted for by normalization alone.

VI. SUMMARY AND DISCUSSION

In this work we have presented a new method for analyzing unresolved spectra of hot, LTE plasmas. The method includes both the UTA and AA models as special, limiting cases. For most situations where the UTA method is impractical and the AA method is not detailed and accurate enough, the STA model provides a tractable, yet accurate analysis. Furthermore, in contrast to the AA model, the approximations of the STA model can be successively improved to obtain convergence. The STA model includes all the contributions to a transition array in terms of only a few tens of superarrays. It allows the identification of the dominant set of configurations, which can then be treated, if necessary, by more detailed UTA or line-by-line calculations. In previous analyses,[12] it was necessary to decide *a priori* which configurations dominate and ignore the rest. We have shown that this procedure cannot be corrected by normalization alone.

We have demonstrated the STA method in two examples. We have shown that the zeroth-order (plus average first-order correction) approximation to energies in the Boltzmann factor is improved for cases where different potentials are taken for different STA's. This can be explained by the fact that the STA potential is obtained by minimizing the first-order superconfiguration average energy (see Appendix B). Finally, we have presented calculations which reconstruct the experimental spectrum from a laser-produced plasma and indicate an application of the method as a plasma diagnostic.

ACKNOWLEDGMENTS

One of us (A. B.-S.) acknowledges fruitful discussions on the subject with B. E. Rozsnyai.

APPENDIX A: RECURSION FORMULAS FOR THE PARTITION FUNCTIONS

The partition function of Eq. (15) is

$$U_Q = \sum_{\{\sum_s q_s = Q\}} \prod_s \begin{bmatrix} g_s \\ q_s \end{bmatrix} X_s^{q_s} , \tag{A1}$$

where

$$X_s = \exp[-(\varepsilon_s - \mu)/kT] \tag{A2}$$

and $\sum_s q_s = Q$. In this appendix we derive two kinds of recursion formulas for the partition function of a supershell σ. For simplicity of notation we omit the subscript σ hereafter.

The first formula, similar to one obtained for the ideal gas,[9] is a recursion over the number of electrons Q_σ in a supershell. It is derived as follows.

We begin by defining the generation function

$$F(z) \equiv \sum_Q z^Q U_Q = \prod_s (1 + zX_s)^{g_s} . \tag{A3}$$

By equating powers of z in the Taylor-series expansion of $F(z)$ we obtain

$$U_Q = F^{(Q)}(z=0)/Q! = (\partial^Q/\partial z^Q) \prod_s (1 + zX_s)^{g_s}|_{z=0} . \tag{A4}$$

Performing the derivatives in Eq. (A4), and defining

$$\chi_n = -\sum_s g_s (-X_s)^n \tag{A5}$$

we obtain

$$\begin{aligned} &U_0(\mathbf{g}) = 1 , \\ &U_1(\mathbf{g}) = F^{(1)}(z=0) = \sum_s g_s X_s F(z)/(1+zX_s)|_{z=0} = \chi_1 , \\ &U_2(\mathbf{g}) = (\chi_1 U_1 + \chi_2)/2 , \\ &U_Q(\mathbf{g}) = \sum_n \chi_n U_{Q-n}(\mathbf{g})/Q . \end{aligned} \tag{A6}$$

Thus the partition functions are obtained in Q steps involving the single set $\{\mathbf{g}\} = (g_1, g_2, \ldots, g_s, \ldots)$, independent of the actual occupation numbers, Q. The partition function (A6) is a formal mathematical function of the set $\{\mathbf{g}\}$, whose elements do not necessarily obey the physical relation $g_s = 2j_s + 1$.

The second recursion formula is over $\{\mathbf{g}\}$:

$$U_Q(\mathbf{g}) = U_Q(\mathbf{g}^\gamma) + X_\gamma U_{Q-1}(\mathbf{g}^\gamma), \tag{A7}$$

where the set $\{\mathbf{g}^\gamma\}$ is obtained from $\{\mathbf{g}\}$ by reducing by 1 the weight of the γ shell, i.e.,

$$\{g_s^\gamma\} = \{g_s - \delta_{\gamma s}\} . \tag{A8}$$

This recursion follows simply from an application of the binomial relation,

$$\begin{bmatrix} g \\ q \end{bmatrix} = \begin{bmatrix} g-1 \\ q \end{bmatrix} + \begin{bmatrix} g-1 \\ q-1 \end{bmatrix} , \tag{A9}$$

in Eq. (A1) for any chosen shell γ, as follows:

$$\begin{aligned} U_Q(\mathbf{g}) &= \sum_{\{\sum_s q_s = Q\}} \prod_s \begin{bmatrix} g_s \\ q_s \end{bmatrix} X_s^{q_s} \\ &= \sum_{\{\sum_s q_s = Q\}} \prod_s \begin{bmatrix} g_s - \delta_{\gamma s} \\ q_s \end{bmatrix} X_s^{q_s} \\ &\quad + \sum_{\{\sum_s q_s = Q\}} \prod_s \begin{bmatrix} g_s - \delta_{\gamma s} \\ q_s - \delta_{\gamma s} \end{bmatrix} X_s^{q_s} . \end{aligned} \tag{A10}$$

It is easily seen that (A10) can be rewritten as Eq. (A7).

APPENDIX B: FIRST-ORDER CONFIGURATION AND SUPERCONFIGURATION AVERAGE ENERGIES

The zero-order energy of a configuration defined as in Eq. (9) is

$$E_C^{(0)} = \sum_{s \in C} q_s \varepsilon_s , \tag{B1}$$

where ε_s is the orbital energy of the s shell. The first-order configuration-average energy is

$$\begin{aligned} E_C^{(1)} &= \sum_{\phi_C} \langle \phi_c | H_0 + H_1 | \phi_C \rangle / g_c \\ &= \sum_{s \in C} q_s \langle s \rangle + \sum_{r,s \in C} q_s (q_r - \delta_{r,s}) \langle r,s \rangle . \end{aligned} \tag{B2}$$

In (B2), H_0 is the central field Hamiltonian, H_1 is the electron-electron interaction Hamiltonian, and

$$g_C = \prod_s \begin{bmatrix} g_s \\ q_s \end{bmatrix}, \quad g_s = 2j_s + 1 . \tag{B3}$$

The one- and two-electron matrix elements are

$$\langle s \rangle = \varepsilon_s + \langle s | -Z/r - V(r) | s \rangle , \tag{B4}$$

$$\begin{aligned} \langle r,s \rangle &= F^{(0)}(r,s) + [g_s/(g_r - \delta_{rs})] \\ &\quad \times \sum_k \begin{bmatrix} j_s & k & j_r \\ \frac{1}{2} & 0 & -\frac{1}{2} \end{bmatrix} G^{(k)}(r,s) , \end{aligned} \tag{B5}$$

where $F^{(k)}$ and $G^{(k)}$ are the usual direct and exchange Slater integrals, respectively.

The average energy of a superconfiguration is defined as

$$E_\Xi^1 \equiv \frac{\sum_{C \in \Xi} g_C E_C^1}{\sum_{C \in \Xi} g_C} . \tag{B6}$$

Using the binomial relation [Eq. (31)] the following expression is obtained:

$$E_\Xi^{(1)} = \sum_{\sigma \in \Xi} Q_\sigma \frac{\sum_{s \in \sigma} g_s \langle s \rangle}{G_\sigma} + \sum_{\sigma,\sigma' \in \Xi} Q_\sigma (Q_\sigma - \delta_{\sigma,\sigma'}) \frac{\sum_{s \in \sigma'} \sum_{s' \in \sigma'} g_s (g_s - \delta_{s,s'}) \langle s,s' \rangle}{G_\sigma (G_\sigma - \delta_{\sigma,\sigma'})} , \tag{B7}$$

where $Q_\sigma = \sum_{s \in \sigma} q_s$ and $G_\sigma = \sum_{s \in \sigma} g_s$ are the supershell occupation number and statistical weight, respectively.

The first-order average correction to the zeroth-order configuration energies is therefore

$$\tilde{E}_\Xi^{(1)} = E_\Xi^{(1)} - \sum_{\sigma \in \Xi} Q_\sigma \frac{\sum_{s \in \sigma} g_s \varepsilon_s}{G_\sigma} \tag{B8}$$

and for the configuration energy in the Boltzmann factor we thus take

$$E_C = \sum_{s \in \sigma} q_s \varepsilon_s + \tilde{E}_\Xi^{(1)} . \tag{B9}$$

APPENDIX C: THE CONFIGURATION TRANSITION ARRAY (UTA) (REF. 1)

Let us denote by $\alpha \equiv \mathbf{j}_\alpha$ and $\beta \equiv \mathbf{j}_\beta$ the initial and final orbitals involved in the radiative transition. The average transition energy between two configurations with $\alpha \rightarrow \beta$, is obtained[1(a)] from Eq. (6), assuming statistical level populations in C:

$$E_C^{(\alpha\beta)} \equiv E_{CC'} = \sum_{s \in C} (q_s - \delta_{s\alpha}) D_s + D_0 , \tag{C1}$$

$$D_0 = \langle \beta \rangle - \langle \alpha \rangle , \tag{C2}$$

$$D_s = \langle s,\beta \rangle - \langle s,\alpha \rangle + \eta(\alpha,\beta)(\delta_{s\beta} - \delta_{s\alpha}) ,$$

where $\eta(\alpha,\beta)$ can be obtained in terms of the Slater integrals $F^{(k)}(\alpha,\beta)$, $G^{(k)}(\alpha,\beta)$, and is independent of q_s. In Eq. (C1) the configuration C' is defined uniquely by $\alpha \rightarrow \beta$, i.e.,

$$C' = \prod_s j_s^{q_s'} , \tag{C3}$$

with $q'_\alpha = q_\alpha - 1$, $q'_\beta = q_\beta + 1$ and $q'_s = q_s$, $s \neq \alpha, \beta$.

The total intensity of the configuration transition array obtained from Eq. (8) is

$$I_{CC'} = kE^3_{CC'} N_C d_C^{(\alpha\beta)} , \tag{C4}$$

where N_C is the total configuration population and

$$d_C^{(\alpha\beta)} = (1/g_C) \sum_{\substack{a \in C \\ b \in C'}} g_a d_{ab} = q_\alpha (g_\beta - q_\beta) r^2_{\alpha\beta}, \tag{C5}$$

$$r^2_{\alpha\beta} = \langle \alpha \| r \| \beta \rangle^2 = (2j_\alpha + 1)(2j_\beta + 1) \begin{bmatrix} j_\alpha & 1 & j_\beta \\ \frac{1}{2} & 0 & -\frac{1}{2} \end{bmatrix}^2 \mathbf{p}^2_{\alpha\beta}, \tag{C6}$$

and $\mathbf{p}_{\alpha\beta}$ is the radial transition integral. The explicit expression for the variance of the configuration transition array is not be needed here.

---

*Permanent address: Nuclear Research Center–Negev, P.O. Box 9001, Beer Sheva 84190, Israel.

[1](a) C. Bauche-Arnoult, J. Bauche, and M. Klapisch, J. Opt. Soc. Am. **68**, 1136 (1978); (b) C. Bauche-Arnoult, J. Bauche, and M. Klapisch, Phys. Rev. A **20**, 2424 (1979); (c) C. Bauche-Arnoult, J. Bauche, and M. Klapisch, Phys. Rev. A **25**, 2641 (1982); (d) C. Bauche-Arnoult, J. Bauche, and M. Klapisch, Phys. Rev. A **30**, 3026 (1984); (e) C. Bauche-Arnoult, J. Bauche, and M. Klapisch, Phys. Rev. A **31**, 2248 (1985); (f) C. Bauche-Arnoult, J. Bauche, and M. Klapisch, Adv. At. Mol. Phys. **23**, 131 (1988); (g) C. Bauche-Arnoult, J. Bauche, M. Klapisch, P. Mandelbaum, and J.-L. Schwob, J. Phys. B **20**, 1443 (1987).

[2]S. D. Bloom and A. Goldberg, Phys. Rev. A **34**, 2865 (1986); **36**, 3152 (1987).

[3]A. Zigler, M. Givon, E. Yarkoni, M. Kishinevsky, E. Goldberg, and B. Arad, Phys. Rev. A **35**, 280 (1987).

[4]J. Stein, D. Shalitin, and Akiva Ron, Phys. Rev. A **31**, 446 (1985).

[5]D. Shvarts (unpublished).

[6]I. I. Sobel'man, *Introduction to the Theory of Atomic Spectra* (Pergamon, Oxford, 1972).

[7]The relativistic extension to this matrix element is given in I. P. Grant, J. Phys. B **7**, 1458 (1974).

[8]J. C. Stewart and K. D. Pyatt, Astrophys. J. **144**, 1203 (1966).

[9]P. T. Landsberg, *Thermodynamics* (Interscience, New York, 1961).

[10]RELAC is a relativistic version of the parametric potential-based atomic structure program MAPPAC; M. Klapisch, Comput. Phys. Commun. **2**, 239 (1971). RELAC was introduced and described by M. Klapisch, J. L. Schwob, B. S. Fraenkel, and J. Oreg, J. Opt. Soc. Am. **61**, 148 (1977).

[11]B. F. Rozsnyai (private communication).

[12]A. Goldberg, B. F. Rozsnyai, and P. Thompson, Phys. Rev. A **34**, 421 (1986).